A new aluminium silicon carbide formed in laser processing

C. HU, T. N. BAKER
Metallurgy and Engineering Materials Group, University of Strathclyde, Glasgow, G1 1XN, UK

During laser processing to create an Al–SiC_p surface metal matrix composite (MMC) layer on AA6061 Al alloy, needle-shaped particles were formed when a high laser energy input was used. Optical microscopy showed this phase to be similar to Al_4C_3 and Al_4SiC_4. Previous work was unable to identify the compound as one of those already known in the Al–Si–C system that included Al_4C_3, Al_4SiC_4, Al_8SiC_7, $Al_4Si_2C_5$ and $Al_4Si_3C_6$. Therefore, in the present work a phase identification was undertaken on the unknown, using transmission electron microscope (TEM) and the associated energy dispersion analytical X-ray (EDAX) system, together with X-ray diffractometry (XRD). This suggested that the phase was an aluminium silicon carbide having an hexagonal structure with $a = 0.3316$ and $c = 2.1330$ nm, which could be a metastable phase formed under the particular laser processing conditions used.

1. Introduction

The successful use of a high power continuous CO_2 laser for the surface treatment of aluminium alloys has been impeded by difficulties in coupling the laser to the material due to high reflectivity, which led to problems with reproducibility of the microstructure and therefore properties [1]. This problem is somewhat overcome with highly alloyed aluminium alloys, such as cast Al–Si alloys [2, 3] and to a much greater extent by incorporating ceramic particles, initially as a surface layer, with a stronger coupling capacity than aluminium [4–10]. The injection of ceramic particles, such as SiC or Al_2O_3, using the protective gas as a carrier has been explored [11–13]. Under specific processing conditions with the technique of preplacement of SiC particulate (SiC_p), a smooth and uniformly thick MMC layer was obtained on the surface of the base alloys, and SiC_p was well distributed in the MMC, with a small amount of Al_4C_3 needles formed at the SiC_p [7]. When a high level of laser energy was used with either preplacement or injection techniques, a complex microstructure was developed, which included SiC particles, Al_4C_3 needles, Al_4SiC_4 platelets and free silicon particles.

Four aluminium silicon carbides have been identified in the literature. Al_4SiC_4 ($Al_4C_3.SiC$) was first reported by Barczak [14], and confirmed in [15–18]. Al_8SiC_7 ($2Al_4C_3.SiC$) was reported by Kidwell *et al.* [19], and confirmed by Oden and McCune [17]. $Al_4Si_2C_5$ ($Al_4C_3.2SiC$) was reported by Inoue *et al.* [20], but was not confirmed by Oden and McCune [17] nor Viala *et al.* [13] and $Al_4Si_3C_6$ ($Al_4C_3.3SiC$) was reported by Oscroft *et al.* [21]. The existence of these phases in the Al–Si–C system together with a wide temperature range developed in the base alloy during laser processing, suggested that Al_8SiC_7, $Al_4Si_2C_5$ and $Al_4Si_3C_6$ may have formed during the process as well as Al_4C_3 and Al_4SiC_4. Therefore, the present work was undertaken to characterize relatively small volume fractions of fine precipitates using analytical TEM complemented with XRD.

2. Experimental procedure

AA6061 Al alloy was used as the base alloy. The composition was Fe 0.21%, Si 0.7%, Mg 1.02%, Cu 0.27%, Mn 0.04%, Cr 0.2% and the balance Al, all in weight per cent. The base alloy specimens had thicknesses of 6–8 mm. A continuous CO_2 5 kW laser (CL5) at Culham Laboratory, AEA Technology, Abingdon with a stationary beam producing a near-field annular energy profile was used for the experiments. The specimens were moved under the beam on a work-table to develop all the tracks processed in the present work. The laser beam power, q, set at 2.8 kW, the radius of the laser beam, r_B, 1.0–2.5 mm, and the velocity of the specimen, v, 5–30 mm s^{-1} were the parameters explored in the processing. The laser energy density is given as $E = q/(r_B v)$ (MJ m^{-2}), referred to as the energy intensity [22]. When the preplacement technique was used, SiC_p (6 and 45 μm), or a mixture of 20–60% of the SiC_p and prealloyed AA6061 powder (40 μm), was blended with an organic solution, and painted on the surface prior to laser scanning. Pure dry argon was used at 50 l min^{-1} to protect the area scanned by the laser. With the injection technique, SiC_p (150 μm) was used as the reinforcement. A mixture of SiC_p (40%) and AA6061 powder (60%, 40 μm) was injected on the preplaced mixture of SiC_p (60%, 6 μm) and AA6061

0022–2461

(40%, 40 μm) on the surface. A powder feeder (Plasma Technik, Twin 10C) with a feeding rate of 5–10 g min^{-1} was used for injecting. Pure dry argon that flowed through a nozzle of 2 mm in internal diameter, was used to carry and to protect both the powder and the laser glazing area against oxidation.

Transverse sections of the laser treated specimens were examined using optical microscopy. The surface was examined with XRD. The XRD analysis was conducted in a Bragg–Brentano geometry using CuK_α radiation, and 40 kV and 20 mA were the settings for the XRD analysis, scanning the 2θ range from 30 to 80° in steps of 0.1°. Each step was recorded for 20 s. A 1 mm thick sheet was cut from the laser treated surface for preparation of thin foils, which were examined using a Philips EM400 TEM and the associated EDAX 9100/600 system.

3. Results and discussion

3.1. Optical microstructure

When a high laser energy density was used with either the preplacement or the injection techniques, complex microstructures were obtained on the surface of the base alloy. A typical micrograph ($E = 280$ MJ m^2) is shown in Fig. 1. SiC_p reacted with, or dissolved into, the matrix. Al_4SiC_4 (dark grey platelets), Al_4C_3 (black needles) and free silicon (grey particles) formed. The dark grey Al_4SiC_4 platelets were identified by EDAX associated with TEM [9], as were the black Al_4C_3 needles [10]. There are two areas in Fig. 1. The one above the line Y–Z shows fewer SiC_p particles and more free Si and Al_4SiC_4, and the region below Y–Z more SiC_p and Al_4C_3 needles. Because the upper area was closed to the laser, it would be expected that during the laser processing this area would in general be at a higher temperature than the area below Y–Z. These observations are in good agreement with the work by Viala *et al.* [18], who reported Al_4C_3 to form from liquid ($L \rightarrow Al_4C_3 + SiC$) in the temperature range 940–1620 K, and Al_4SiC_4 ($4Al + 4SiC \rightarrow Al_4SiC_4 + 3Si$) at temperatures higher or equal to 1670 K. One difference between the microstructures resulting from the preplacement and the injection techniques is that cracks were found in some large SiC particles within the injected MMC layer, but not in the preplaced MMC. This is because SiC_p has a high laser energy absorption, and when SiC_p is laser glazed during injecting, the energy absorbed by SiC_p would not be transferred efficiently to the surroundings due to too few contacts between SiC_p and AA6061 particles, and therefore the SiC_p was rapidly heated. The rapid decrease in temperature and the high temperature reached, would result in a dramatic increase in the internal stress of the SiC_p and therefore cause the cracks in the largest SiC_p.

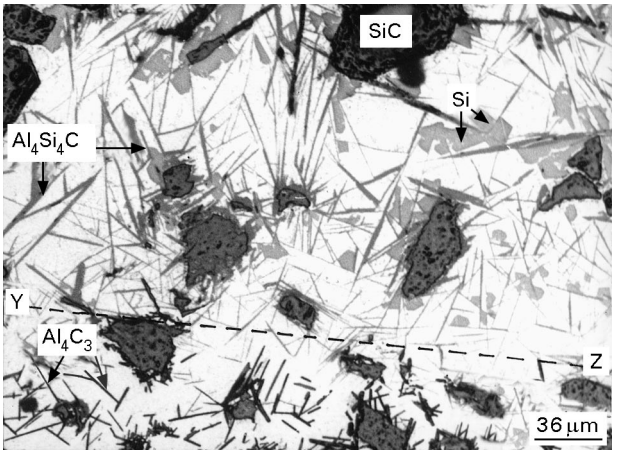

Figure 1 Microstructure obtained when a high laser energy density ($E = 280$ MJ mm^{-1}) was used with the injection technique.

It is noted that many of the grey needles formed in the upper area in Fig. 1 are morphologically similar to, but seem to be a different phase from either Al_4SiC_4 or Al_4C_3. They could be any of the phases mentioned above, or indeed a new phase. Therefore, a further phase identification was undertaken.

3.2. XRD and TEM analysis

The MMC layer shown in Fig. 1 was examined by XRD. An example of the spectrum is given in Fig. 2. The peaks from SiC, Si and Al in Fig. 2 confirm that there are SiC and silicon in the aluminium matrix. But the other peaks labelled A, B, C and D do not fit the peaks expected from the Al_4C_3, Al_4SiC_4, Al_8SiC_7, $Al_4Si_2C_5$ or $Al_4Si_3C_6$ phases. In fact, all the possible sets of two peaks of those labelled A, B, C and D failed to fit any of the already known phases. From Fig. 1, Al_4C_3 needles formed in the area in a distance below the surface, which is beyond the region detectable by XRD. When a low laser energy density was used ($E = 140$ MJ m^{-2}), the Al_4C_3 needles formed in the upper region of the surface, and were identified using XRD in our previous work [9]. The reason for the omission of the expected peaks from the Al_4SiC_4 phase in Fig. 1 is due to the small amount of the phase in the upper region that reflected signals that were too weak to be recorded. However, the existence of the Al_4SiC_4 phase in the top region has also been identified previously [7]. Both the large quantity of the long grey needles in the top region and the unidentified peaks in the XRD spectrum suggest that this phase in upper areas in Fig. 1 has not been identified previously, and that it may be one of the phases formed in the MMC layer that underwent a structural distortion during cooling following laser processing. In the following discussion, this unknown phase is called ASC.

Foils, obtained from the same area of the specimen shown in Fig. 1 where the unknown phase was noted, were examined using TEM, and a typical micrograph is shown in Fig. 3. The electron diffraction pattern from the region indicated as (S) in Fig. 3, is given in Fig. 4a, showing an orientation relationship of the ASC phase with the aluminium matrix. A second electron diffraction pattern from the same particle as that given in Fig. 4a, but in a different orientation obtained after tilting the specimen, is given in Fig. 5a. The structures, the lattice parameters and the three strongest peaks from standard JCPDS data of the possible phases in the Al–Si–C system, which have been identified in the literature, are given in Table I.

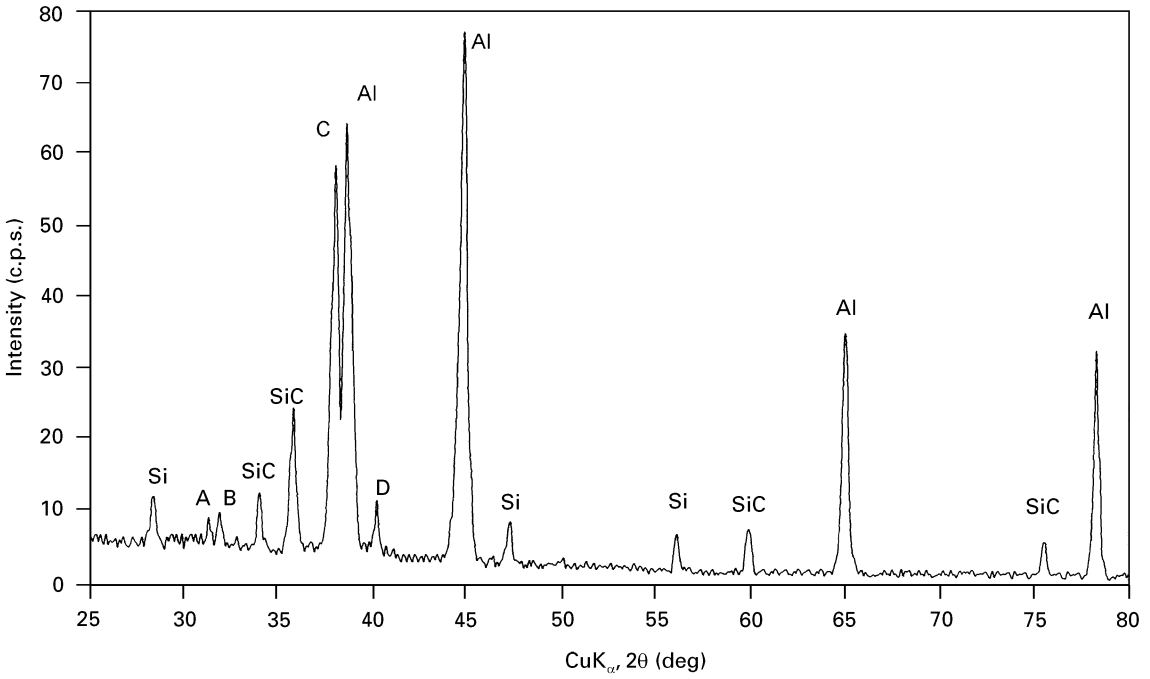

Figure 2 The XRD spectrum from the MMC layer shown in Fig. 1.

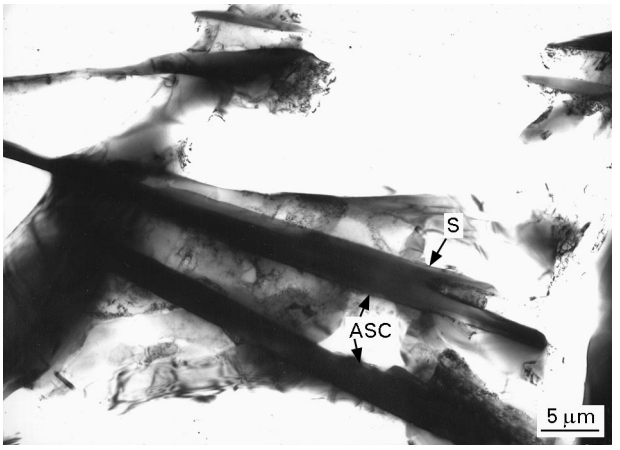

Figure 3 A TEM photograph obtained from the upper area in Fig. 1, showing the needle particles in the Al matrix.

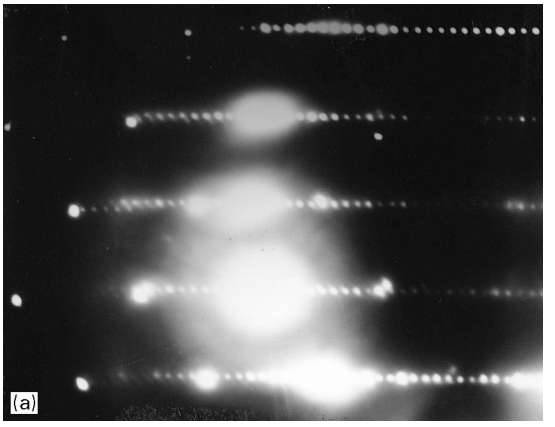

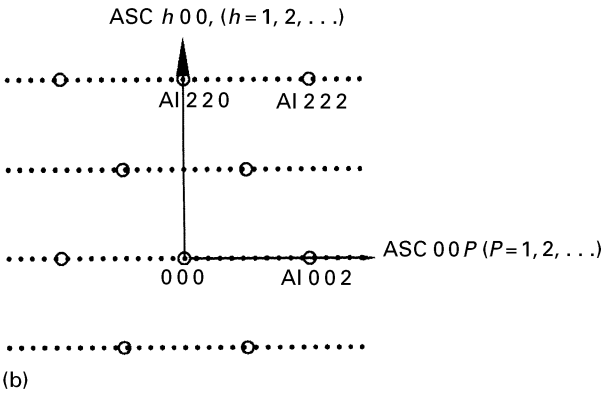

Figure 4 (a) An electron diffraction pattern obtained from the region specified (S) in Fig. 3, and (b) a schematic interpreted electron diffraction pattern of (a) (○) Al, (·) ASC.

The electron diffraction patterns from the ASC particle, in Figs 4a and 5a, could not be interpreted from the data established for Al_4C_3, Al_4SiC_4, Al_8SiC_7, $Al_4Si_2C_5$ or $Al_4Si_3C_6$. This is strong evidence for the ASC particles in Fig. 4 being considered as the same phase that provided the unidentified peaks labelled A, B, C and D in Fig. 2. There is another possibility that one of peaks A, B, C and D could be obtained from one of the already known phases, and the rest from the phase ASC. In this case, the peak from the known phase may be that having the highest intensity as listed in Table I, when the second highest intensity peak was too weak to be recorded because of the small quantity of the phase formed in the upper region. Several identical spectra and diffraction patterns were obtained from other identical samples.

The pattern from the aluminium matrix in Fig. 4a was used to obtain the camera constant, and therefore to calibrate the pattern from the ASC phase, which does not fit a cubic structure. With an hexagonal structure, the interpretation of the patterns in Figs 4a and 5a is schematically given in Figs 4b and 5b, respectively. The calculation from the data obtained from the patterns gives the lattice parameters $a = 0.331$ and $c = 2.14$ nm. Using this data to interpret the X-ray spectra, peak A in Fig. 2 was considered

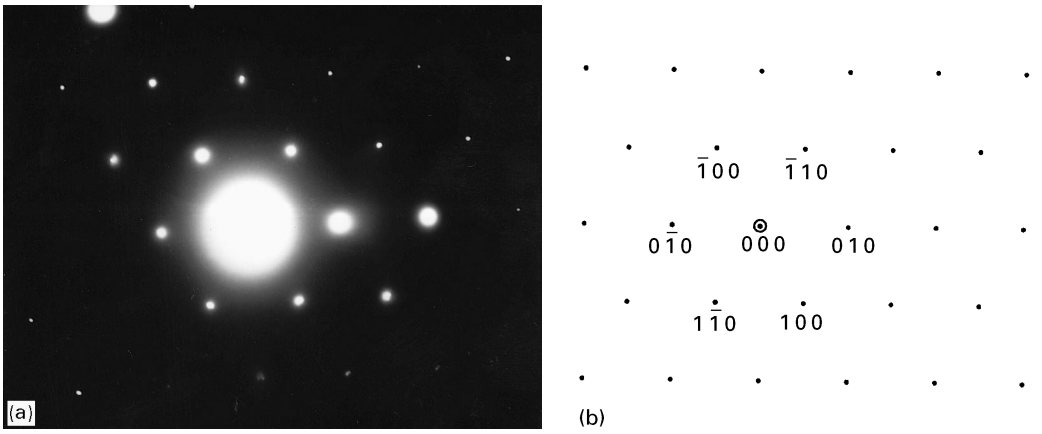

Figure 5 (a) An electron diffraction pattern obtained from the same region as Fig. 4 but with a different orientation after tilting, and (b) a schematic interpreted electron diffraction pattern of (a).

TABLE I Some related data of the previously identified phases in the AlSi–C system

Phases	Structures	Lattice parameters		Expected three strongest peaks from standard JCPDS data					
		a (nm)	c (nm)	(hkl)	I/I_1	(hkl)	I/I_1	(hkl)	I/I_1
Al_4C_3	Hexagonal	0.3331	2.499	(1 0 0)	100	(0 1 2)	60	(1 0 7)	60
Al_4SiC_4	Hexagonal	0.656	1.080	(1 1 2)	100	(2 0 3)	65	(2 2 0)	60
Al_8SiC_7	Hexagonal	0.3313	1.924	(0 0 9)	100	(0 0 7)	23	(0 0 5)	20
$Al_4Si_2C_5$	Hexagonal	0.425	4.011	(1 0 11)	100	(1 0 18)	100	(1 0 12)	90
$Al_4Si_3C_6$	Hexagonal	0.3232	3.178	(1 0 0)	100	(1 1 0)	100	(1 0 2)	50

to be associated with the (1 0 0) plane, C with (0 0 9) and D with (1 0 6), which give the corresponding 2θ values of 31.2° (error = 0.32%), 37.80 (error = 0.53%) and 40.3° (error = 0.25%), respectively. Peak B still cannot be assigned any d-spacings of the ASC phase. It is noted that peak B is located at the expected 2θ value (31.9°) of the (1 1 2) peak of Al_4SiC_4, which is the strongest peak for this compound quoted in the standard JCPDS data. Therefore, peak B is considered to be associated with the Al_4SiC_4 particles formed in the surface. Other peaks expected from the Al_4SiC_4 particles were too weak to be recorded because of a small volume of the phase in the surface. However, these particles are present in the upper region of Fig. 1.

Because an XRD analysis is expected to give a more accurate result than that obtained from the electron diffraction patterns, a least-square computer program was used to obtain the lattice parameters from the 2θ values of peaks A, C and D. This gives $a = 0.3316$ and $c = 2.1330$ nm, which are in good agreement with the electron diffraction data exemplified in Figs 4a and 5a, with errors of 0.18 and 0.03% for a and c, respectively.

Fig. 4a also shows an orientation relationship of $[0\,1\,\bar{1}\,0]_{ASC} \parallel [1\,1\,0]_{Al}$, $(1\,0\,\bar{1}\,0)_{ASC} \parallel (1\,1\,0)_{Al}$ and $(0\,0\,0\,1)_{ASC} \parallel (0\,0\,1)_{Al}$. The interplanar spacings of $(1\,0\,\bar{1}\,0)_{ASC}$ and $(1\,1\,0)_{Al}$ are 0.2872 and 0.2864 nm, respectively, from the calculation and a good continuity between the ASC phase and the Al matrix would be expected.

The EDAX spectra from the ASC phase indicated that it is an aluminium silicon carbide compound. The quantitatively analytical software associated with EDAX was used to obtain the Al : Si atomic ratio, and an average of five values from different particles of the same phase was used. The average Al : Si atomic ratio in the compound was 3.52. Unfortunately, because of the difficulty of obtaining pure crystals of ASC, a more accurate composition of ASC was not possible in the present work. Comparing the Al : Si ratio with all the known aluminium silicon carbides, the ASC phase was not in agreement with any that have the same composition but a different crystal structure. Since the ASC phase has not been identified by previous researchers, it is more likely to be a metastable phase that forms under the particular conditions of laser processing. It is noticed that the Al : Si ratio of Al_4SiC_4, compared with the other possible compounds, is closest to that of the ASC phase (4.00 compared with 3.52), and also that an aluminium silicon carbide with the Al_4SiC_4 composition was identified by Inoue *et al.* [20], to have an hexagonal lattice with $a = 0.32771$ and $c = 2.1676$ nm, which are similar to those of the ASC phase obtained in the present work. Furthermore, the ASC phase formed in the same area as the Al_4SiC_4 phase, shown in Fig. 1. This suggests that the ASC and Al_4SiC_4 compounds formed in the same temperature range, which is higher than that for Al_4C_3. Therefore, the ASC phase could be a solid solution of Al_4SiC_4 with more silicon atoms dissolved in the phase when a high silicon content and rapid cooling rate coexist.

4. Conclusions

1. A previously unknown aluminium silicon carbide has been identified after laser processing of AA6061 and preplaced SiC_p. XRD analysis and selected area electron diffraction patterns suggest that

this phase has an hexagonal structure with $a = 0.3316$ and $c = 2.1330$ nm.

2. This aluminium silicon carbide could be a metastable phase that forms under the particular conditions of laser processing. The presence of a high silicon content may be necessary for the formation of this compound.

3. The orientation relationship obtained from electron diffraction patterns of thin foils, $[0\,1\,\bar{1}\,0]_{ASC} \parallel [1\,1\,0]_{Al}$, $(1\,0\,\bar{1}\,0)_{ASC} \parallel (1\,1\,0)_{Al}$ and $(0\,0\,0\,1)_{ASC} \parallel (0\,0\,1)_{Al}$, and the close interplanar spacings, 0.2872 nm for $(1\,0\,\bar{1}\,0)_{ASC}$ and 0.2864 nm for $(1\,1\,0)_{Al}$ (based on the calculation), both indicate a good continuity between this phase and the Al matrix.

Acknowledgements

The authors would like to thank the Defense Research Agency for the main financial support for this work, and the late Professor A. W. Bowen at DRA Farnborough, for advice and useful discussions.

References

1. C. W. DRAPER and J. M. PROATE, *Int. Met. Rev.* **30** (1995) 85.
2. A. M. WALKER, W. M. STEEN and D. R. F. WEST, in "Aluminium technology", edited by T. Sheppard (Institute Metals, London, 1986) p. 712.
3. H. WOLLMER and E. HORNBOGEN, in "Treatment of materials", edited by B. L. Mordike (D. G. M. Information, Institute for Metals, London, 1987) p. 163.
4. N. B. DAHOTRE, T. D. MCCAY and M. H. MCCAY, *J. Appl. Phys.* **65** (1989) 5072.
5. A. G. CROOKS and E. HORNBOGEN, *Metall.* **43** (1989) 957.
6. T. N. BAKER, H. XIN, C. HU and S. MRIDHA, *Mater. Sci. Technol.* **10** (1994) 536.
7. C. HU and T. N. BAKER, *J. Mater. Sci.* **30** (1995) 891.
8. C. HU, L. BARNARD, S. MRIDHA and T. N. BAKER, *J. Mater. Pro. Technol.* **58** (1996) 87.
9. C. HU, H. XIN and T. N. BAKER, *Mater. Sci. Technol.* **12** (1996) 227.
10. X. B. ZHOU and J. T. M. DE HOSSON, *Scripta Metall. Mater.* **28** (1993) 219.
11. J. D. AYERS, R. J. SCHAEFER and W. P. ROBEY, *J. Met.* **33** (1981) 19.
12. P. SALLAMAND and J. M. PELLETIER, *Mater. Sci. Eng.* **A171** (1993) 263.
13. C. HU, H. XIN and T. N. BAKER, *J. Mater. Sci.* **30** (1995) 5985.
14. V. J. BARCZAK, *J. Amer. Ceram. Soc.* **44** (1961) 299.
15. J. SCHOENNAHL, B. MILLER and M. DAIRE, *J. Mater. Sci.* **4** (1979) 338.
16. G. SCHNEIDER, L. J. GAUCKLEV, G. PETZOW and A. ZANGVIL, *ibid.* **62** (1979) 574.
17. L. L. ODEN and R. A. MCCUNE, *Metall. Trans. A* **18** (1987) 2005.
18. J. C. VIALA, P. FORTIER and J. BOUIX, *J. Mater. Sci.* **25** (1990) 1842.
19. B. L. KIDWELL, L. L. ODEN and R. A. MCCUNE, *J. Appl. Crystallog.* **17** (1984) 481.
20. Z. INOUE, Y. INOMATA, H. TANAKA and H. KAWABATA, *J. Mater. Sci.* **15** (1980) 575.
21. R. OSCROFT, P. KORGUL and D. THOMPSON, *Brit. Ceram. Proc.* **42** (1992) 33.
22. M. F. ASHBY and K. E. EASTERLING, *Acta. Metall.* **32** (1984) 1935.

Received 27 January
and accepted 26 February 1997